The influence of droplet size on line tension

2004 J. Phys.: Condens. Matter 16 6917

(http://iopscience.iop.org/0953-8984/16/39/024)

INSTITUTE OF PHYSICS PUBLISHING JOURNAL OF PHYSICS: CONDENSED MATTER

J. Phys.: Condens. Matter **16** (2004) 6917–6928 PII: S0953-8984(04)82453-6

The influence of droplet size on line tension

P Jakubczyk[1] **and M Napiórkowski**

Instytut Fizyki Teoretycznej, Uniwersytet Warszawski, 00-681 Warszawa, Hoża 69, Poland

E-mail: Pawel.Jakubczyk@fuw.edu.pl

Received 21 June 2004, in final form 10 August 2004
Published 17 September 2004
Online at stacks.iop.org/JPhysCM/16/6917
doi:10.1088/0953-8984/16/39/024

Abstract

Within the effective interfacial Hamiltonian approach we evaluate the excess line free energy associated with hemicylindrical droplets of volatile liquid sessile on a stripe-like chemical inhomogeneity of a planar substrate. In the case of short-range intermolecular forces the droplet morphology and the corresponding expression for the line tension—which includes the inhomogeneity finite width effects—are derived and discussed as functions of temperature and increasing width. The width-dependent contributions to the line tension change their structure at the stripe wetting temperature T_{W1}: for $T < T_{W1}$ they decay exponentially while for $T > T_{W1}$ the decay is algebraic in the heterogeneity width. In addition, a geometric construction of the corresponding contact angle is carried out and its implications are discussed.

1. Introduction

A lot of theoretical and experimental effort has recently been made towards understanding adsorption on substrates equipped with geometric and chemical structure. This research exposed a variety of phenomena and associated problems, such as the filling transitions [1–4], the position and droplet's size-dependent contact angles and interfacial morphology structures [5–10], discontinuous changes in droplet shapes as a function of volume [11, 12], or the influence of the substrate's structure on the existence and order of wetting transitions as compared to the homogeneous and planar substrate case [13–17]. In many such systems the interfacial morphology leads to the existence of three-phase contact lines and in consequence to the line tension [18]. This quantity's properties, and especially its behaviour close to the wetting transitions, stimulated many discussions and gave rise to controversies in recent years [19–30].

In this paper we are concerned with a semi-infinite fluid in a thermodynamic state close to its bulk liquid–vapour coexistence, in the presence of a substrate consisting of a single stripe-like inhomogeneity placed on an otherwise chemically homogeneous and planar solid surface;

[1] Author to whom any correspondence should be addressed.

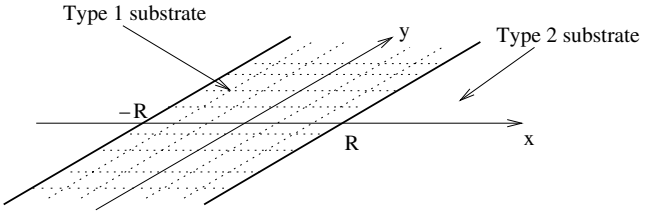

Figure 1. A schematic illustration of a planar substrate containing a stripe-like inhomogeneity. The wetting temperature of the stripe (T_{W1}) is assumed lower than the substrate 2 wetting temperature (T_{W2}). The domain width ($2R$) is considered to be much larger than bulk correlation lengths.

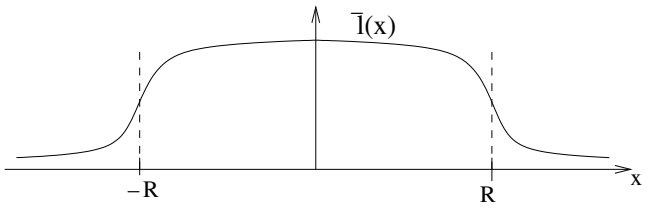

Figure 2. Schematic plot of the $y = \text{const}$ section of the equilibrium shape of the liquid–vapour interfacial profile $\bar{l}(x)$.

see figure 1. The system is translationally invariant along the stripe, say in the y-direction, and the equilibrium adsorption morphology varies only in the x-direction perpendicular to the stripe, the width of which is denoted by $2R$. Thus the chemical inhomogeneity of the substrate imposes non-uniformity of the liquid-like layer adsorbed at the substrate. Its thickness varies in the x-direction and induces a linear contribution to the fluid free energy. This contribution evaluated per unit length of the stripe will be denoted η, and called the line tension. It is a function of temperature T, the inhomogeneity width $2R$, and additionally depends on quantities characterizing both the stripe and the rest of the substrate. These additional quantities will be represented by the relevant wetting temperatures of two parts of the substrate. The $y = \text{const}$ section of the system can be looked upon as a two-dimensional droplet of volatile liquid sessile on a one-dimensional substrate inhomogeneity; see figure 2. We are particularly interested in contributions to the droplet line tension resulting from its finite size—their dependence on temperature and the heterogeneity width.

In addition to analysing the droplet morphology and the contributions to the line tension we perform geometric constructions of the relevant contact angles. These constructions correspond to different choices of the three-phase contact line and lead to different predictions concerning the behaviour of the contact angle in the limit $R \to \infty$. In effect, only one of them turns out to have practical meaning.

This work is arranged as follows. In section 2 we specify the model and discuss its limitations. A set of constrained equilibrium profiles parameterized by the droplet height at its centre is constructed and the constrained excess line free energy expressions as functions of the droplet height, inhomogeneity width $2R$, temperature, and the corresponding wetting temperatures, are derived. In section 3 we construct the expansion for equilibrium droplet height in the limit of large R. We recover some of the earlier specific results [31] together with new expressions for the corrections up to the order which is necessary to calculate the leading R-dependent contributions to the line tension. In section 4 the expressions for the line tension are derived and discussed. In section 5 we analyse the contact angles obtained from the equilibrium liquid–vapour interfacial shapes.

2. The model

We consider a planar, chemically inhomogeneous substrate remaining in contact with a fluid. The system's thermodynamic state is infinitesimally close to the fluid's bulk liquid–vapour coexistence, i.e., $\mu = \mu_{\rm sat}^{-}$, where $\mu_{\rm sat}$ denotes the chemical potential at liquid–vapour coexistence. The inhomogeneity has the form of a stripe of width $2R$. The substrate is translationally invariant in the y-direction defined by the inhomogeneity's orientation; see figure 1. The wetting temperature of the stripe, $T_{\rm W1}$, is lower than that of the remaining part of the substrate, $T_{\rm W2}$, i.e., $T_{\rm W1} < T_{\rm W2}$, so that the liquid phase is preferentially adsorbed on the stripe. The system's temperature T is assumed to be lower than $T_{\rm W2}$ so that the equilibrium thickness of the adsorbed layer $\bar{l}(x)$ converges in the limit $x \to \pm\infty$ to a finite value determined by the properties of substrate 2 alone; see figure 2.

A suitable description of this system, valid on length scales much larger than the bulk correlation length $\xi_{\rm B}$, is provided by the interfacial Hamiltonian model [32, 33]

$$\mathcal{H}[l] = \int {\rm d}x \int {\rm d}y \left[\frac{\sigma}{2} (\nabla l)^2 + V(l, x) \right]. \tag{2.1}$$

Here $l(x, y)$ denotes the interface position, σ the liquid–vapour surface tension, and $V(l, x)$ the effective interfacial potential. The borderline between substrates of types 1 and 2 is assumed to be of the order of $\xi_{\rm B}$, and the crossover in $V(l, x)$ is anticipated to occur over a distance of the same magnitude for systems with short-range intermolecular forces [31, 32]. Consequently, we model $V(l, x)$ as

$$V(l, x) = \Theta(R - |x|) V_1(l) + \Theta(|x| - R) V_2(l), \tag{2.2}$$

where $V_1(l)$ and $V_2(l)$ are the effective interfacial potentials corresponding to homogeneous substrates of type 1 and 2, respectively, and $\Theta(x)$ is the Heaviside step function. The consequences of approximating the continuous potential $V(l, x)$ by the steplike form in equation (2.2) were shown to be negligible for the interfacial structure in the case of long-range forces (see [8]). We expect this conclusion of [8] to be valid for systems with short-range interactions as well. In this case each of the potentials $V_i(l)$ ($i = 1, 2$) has the exponential form (see e.g., [16, 31])

$$V_i(l) = \tau_i {\rm e}^{-l/\xi_{\rm B}} + b {\rm e}^{-2l/\xi_{\rm B}} + \cdots, \tag{2.3}$$

where $\tau_i = a(T - T_{{\rm W}i})$, a being a positive constant, and $\xi_{\rm B}$ denotes the bulk correlation length in the adsorbed liquid phase. The positive parameter b controls repulsion of the interface from the substrate at short distances. For simplicity, within our model, it has the same value for substrates of both kinds.

Throughout this work we apply the mean-field approach according to which the equilibrium grand canonical average value of the adsorbed layer's thickness $\langle l(x) \rangle$ is identified with $\bar{l}(x)$ which minimizes the Hamiltonian (2.1). This approximation neglects interfacial fluctuations. Although the upper critical dimension for the wetting of homogeneous substrates in the case of short-range forces is $d_u = 3$, it was argued in [31] for the present inhomogeneous system that asymptotically for $x \approx 0$, $R/\xi_{1\|} \gg 1$ the net result of incorporating fluctuations amounts to replacing $\xi_{\rm B}$ with an effective correlation length. However, one cannot exclude additional effects caused by thermal fluctuations in the vicinity of substrate's inhomogeneity, which are not taken into account in this paper. One should also note that the full drumhead expression in the interfacial Hamiltonian (see e.g., [34]) is substituted with the gradient term in (2.1). This approximation is valid for small differences between both substrates, which in turn is controlled by the difference $\tau_1 - \tau_2$. The equilibrium profile $\bar{l}(x, y)$ is invariant with

respect to translation in the y-direction and in addition $\bar{l}(x, y) = \bar{l}(x) = \bar{l}(-x)$. From now on the considered values of x are limited to $x \in [0, \infty[$.

Minimizing the functional (2.1) leads to the Euler–Lagrange equation

$$\sigma \frac{\mathrm{d}^2 l}{\mathrm{d}x^2} = \frac{\mathrm{d}V}{\mathrm{d}l} \tag{2.4}$$

together with the derivative continuity condition

$$\left.\frac{\mathrm{d}l}{\mathrm{d}x}\right|_{x=R^-} = \left.\frac{\mathrm{d}l}{\mathrm{d}x}\right|_{x=R^+}. \tag{2.5}$$

The minimization procedure is performed in two steps. First we solve equation (2.4) subject to the boundary conditions: $\frac{\mathrm{d}l}{\mathrm{d}x}|_{x=0} = 0$, $\lim_{x\to\infty} l(x) = l_{\pi 2}$, where $l_{\pi 2}$ corresponds to the minimum of $V_2(l)$. The droplet height at the centre $l_0 = l(x = 0)$ is for the time being kept as a fixed but arbitrary parameter. This way we obtain a set of constrained equilibrium profiles denoted by $\{\tilde{l}(x, l_0)\}$; they are parameterized by l_0. In the second step the equilibrium droplet height $\bar{l}_0$ and thus $\bar{l}(x) = \tilde{l}(x, \bar{l}_0)$ are determined by minimizing $H[\tilde{l}(x, l_0)]$ with respect to l_0.

For this purpose two cases must be distinguished: (1) $V_1(l_0) < 0$; and (2) $V_1(l_0) \geqslant 0$. In case (1), upon applying (2.2), (2.3) we obtain the following formulae for the constrained equilibrium profiles corresponding to fixed value l_0:

$$\frac{\tilde{l}(x, l_0)}{\xi_{\mathrm{B}}} = \begin{cases} \log\left[\dfrac{1}{2V_1(l_0)}\left(\tau_1 + (\tau_1 + 2b\mathrm{e}^{-l_0/\xi_{\mathrm{B}}})\cosh\left(\sqrt{\dfrac{-2V_1(l_0)}{\sigma}}\dfrac{x}{\xi_{\mathrm{B}}}\right)\right)\right] & \text{for } x \leqslant R \\ \log\left[\dfrac{2b}{\tau_2}\left(-1 - \exp\left(\dfrac{\tau_2}{\sqrt{2\sigma b}}(x - C)/\xi_{\mathrm{B}}\right)\right)\right] & \text{for } x > R; \end{cases} \tag{2.6}$$

whilst for case (2) we have

$$\frac{\tilde{l}(x, l_0)}{\xi_{\mathrm{B}}} = \begin{cases} \log\left[\dfrac{1}{2V_1(l_0)}\left(\tau_1 + (\tau_1 + 2b\mathrm{e}^{-l_0/\xi_{\mathrm{B}}})\cos\left(\sqrt{\dfrac{2V_1(l_0)}{\sigma}}\dfrac{x}{\xi_{\mathrm{B}}}\right)\right)\right] & \text{for } x \leqslant R \\ \log\left[\dfrac{2b}{\tau_2}\left(-1 - \exp\left(\dfrac{\tau_2}{\sqrt{2\sigma b}}(x - C)/\xi_{\mathrm{B}}\right)\right)\right] & \text{for } x > R. \end{cases} \tag{2.7}$$

For an example plot see figure 3. The above expressions are valid for $x \geqslant 0$ and negative x-values are reached via $\tilde{l}(-x, l_0) = \tilde{l}(x, l_0)$. The constant C is in each case determined by the continuity condition of $\tilde{l}(x, l_0)$ at $x = R$. Note that $\tilde{l}(x = R^-; l_0)$ is uniquely given by l_0. We require that l_0 is such that

$$\tilde{l}(x = R^-, l_0) \geqslant l_{\pi 2}. \tag{2.8}$$

The necessity to make this additional though rather natural assumption is a consequence of the discontinuous form of the interfacial potential $V(l, x)$, see equation (2.2), which allowed us to solve equation (2.4) for $x < R$ and $x > R$ independently. The condition (2.8) implies that the argument of the cosine function in equation (2.7) does not exceed π for $x \in [0, R[$ and therefore the profile given by (2.7) does not exhibit oscillatory behaviour.

The profiles $\tilde{l}(x, l_0)$ are decreasing functions of x, concave for $x < R$ and convex for $x > R$.

At this stage one may calculate the constrained line contribution to the free energy per unit length in the y-direction as a function of l_0 and R; it is defined as

$$H(l_0, R) = \int_0^\infty \mathrm{d}x \left[\frac{\sigma}{2}\left(\frac{\mathrm{d}\tilde{l}(x, l_0)}{\mathrm{d}x}\right)^2 + V(x, \tilde{l}) - V_1(l_{\pi 1})\Theta(R - x) - V_2(l_{\pi 2})\Theta(x - R)\right]. \tag{2.9}$$

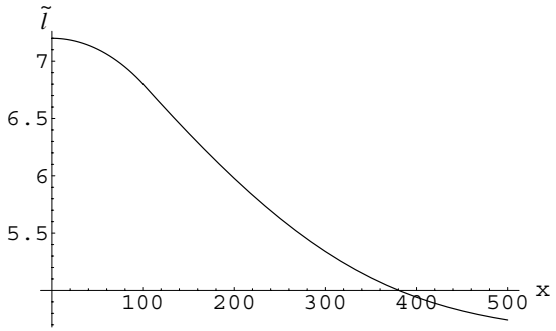

Figure 3. An example of constrained equilibrium droplet profile $\tilde{l}(x, l_0)$. The plot parameters were chosen as follows: $2b/\sigma = 1$, $\tau_1/\sigma = 0.1$, $\tau_2/\sigma = -0.01$. The lengths x, $l_0 = 7.2$, $R = 100$ are expressed in units of ξ_B. The profile's first derivative is discontinuous at $x = R$ (not visible in this figure's scale). The magnitude of the derivative discontinuity decreases to zero for $l_0 \to \bar{l}_0$.

Substituting expression (2.6) for case (1) and (2.7) for case (2) we obtain the following formulae:

$$\begin{aligned}\frac{H(l_0, R)}{\xi_B} = {} & \sqrt{2\sigma b}\left(\frac{\tau_2}{2b} + \frac{2V_1(l_0)}{\tau_1 + (\tau_1 + 2be^{-l_0/\xi_B})\cosh(\alpha)}\right) - V_1(l_0)\frac{R}{\xi_B} \\ & + 2\tau_1\sqrt{\frac{\sigma}{2b}}\operatorname{arth}\left(\sqrt{\frac{b}{-V_1(l_0)}}e^{-l_0/\xi_B}\operatorname{tgh}\frac{\alpha}{2}\right) - \sqrt{-2\sigma V_1(l_0)}\frac{\sinh\alpha}{\frac{\tau_1}{\tau_1+2be^{-l_0/\xi_B}} + \cosh\alpha} \\ & - \sqrt{\frac{\sigma}{2b}}\tau_2\log\left[\frac{-\tau_2}{4bV_1(l_0)}\left(\tau_1 + (\tau_1 + 2be^{-l_0/\xi_B})\cosh(\alpha)\right)\right] + \frac{\tau_1^2}{4b}\frac{R}{\xi_B}\Theta(-\tau_1)\end{aligned} \tag{2.10}$$

for case (1), and

$$\begin{aligned}\frac{H(l_0, R)}{\xi_B} = {} & \sqrt{2\sigma b}\left(\frac{\tau_2}{2b} + \frac{2V_1(l_0)}{\tau_1 + (\tau_1 + 2be^{-l_0/\xi_B})\cos\alpha}\right) - V_1(l_0)\frac{R}{\xi_B} \\ & + 2\tau_1\sqrt{\frac{\sigma}{2b}}\operatorname{arth}\left(\sqrt{\frac{b}{V_1(l_0)}}e^{-l_0/\xi_B}\operatorname{tg}\frac{\alpha}{2}\right) + \sqrt{2\sigma V_1(l_0)}\frac{\sin\alpha}{\frac{\tau_1}{\tau_1+2be^{-l_0/\xi_B}} + \cos\alpha} \\ & - \sqrt{\frac{\sigma}{2b}}\tau_2\log\left[\frac{-\tau_2}{4bV_1(l_0)}\left(\tau_1 + (\tau_1 + 2be^{-l_0/\xi_B})\cos\alpha\right)\right] + \frac{\tau_1^2}{4b}\frac{R}{\xi_B}\Theta(-\tau_1)\end{aligned} \tag{2.11}$$

for case (2), where $\alpha = \sqrt{|\frac{2V_1(l_0)}{\sigma}|}\frac{R}{\xi_B}$. Note that the set of physically relevant values of l_0 is limited by the condition (2.8), which means that $l_0 > l_{0\min}$, where $l_{0\min}$ is given by $\tilde{l}(x = R, l_{0\min}) = l_{\pi 2}$. The inhomogeneity width R is arbitrary; nevertheless, in further calculations we shall assume $\xi_{\|i} \ll R$, where $\xi_{\|i}$ denotes the mean-field interfacial correlation length corresponding to substrate of type $i = 1, 2$, $\xi_{\|i}^{-2} = V_i''(l_{\pi i})/\sigma$.

The formulae (2.6), (2.7), (2.10), and (2.11) form the starting point for the subsequent analysis aiming at the determination of the equilibrium droplet height, line tension, and the contact angles. The line tension η as a function of τ_i and R is given as the minimum of $H(l_0, R)$ with respect to l_0. The corresponding value of the droplet height is denoted by $\bar{l}_0$. Consequently, the equilibrium interfacial shape $\bar{l}(x) = \tilde{l}(x, \bar{l}_0)$, and $\eta = H(\bar{l}_0, R)$.

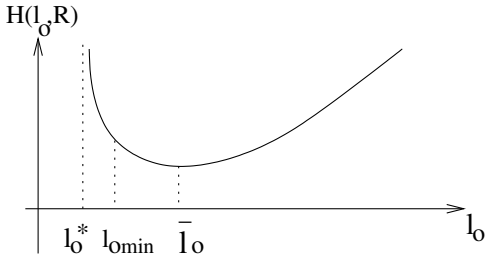

Figure 4. A sketch of $H(l_0, R)$ for fixed R. The physically meaningful values of droplet height fulfil $l_0 > l_{0\,\mathrm{min}}$, where $l_{0\,\mathrm{min}}$ is determined by the condition $\tilde{l}(x = R, l_{0\,\mathrm{min}}) = l_{\pi 2}$. The function $H(l_0, R)$ diverges at $l_0^* < l_{0\,\mathrm{min}}$.

3. The equilibrium droplet height

The scaling behaviour of the equilibrium droplet height $\bar{l}_0$, for $R \to \infty$ and $\tau_1 > 0$, was obtained by Parry *et al* using conformal properties of equation (2.4) in the case $b = 0$ [31]. However, this technique fails when the term $\sim \mathrm{e}^{-2l/\xi_\mathrm{B}}$ in $V_1(l)$ must be taken into account. As we show below, the term neglected in [31] contributes to the corrections to the leading behaviour of $\bar{l}_0$ which are essential to determine the character of the asymptotic expansion of line tension η for large R. In the following subsections we expand the functions $\frac{\partial H(l_0,R)}{\partial l_0}$ around the properly chosen values $l_0^{(0)}$ of l_0 for different temperature ranges. We assume that $\bar{l}_0 = l_0^{(0)} + \delta l_0$, $\delta l_0 \ll l_0^{(0)}$, and solve the appropriate equation for δl_0, thus determining $\bar{l}_0$ up to terms necessary for the calculation of the leading correction to η due to the finite values of R.

3.1. The $\tau_1 > 0$ regime

In this case the numerical analysis of the constrained line tension $H(l_0, R)$ given by equation (2.11) shows that the equilibrium droplet height fulfils the condition $\alpha(\bar{l}_0(R)) \to \pi^-$, as $R \to \infty$. The range of physically relevant values of l_0 is limited by the condition (2.8). It follows that only $l_0 > l_{0\,\mathrm{min}}$ should be considered, where $l_{0\,\mathrm{min}}$ is defined by $\tilde{l}(x = R, l_{0\,\mathrm{min}}) = l_{\pi 2}$. We note that $H(l_0, R)$ diverges at $l_0 = l_0^* < l_{0\,\mathrm{min}}$ and one can check that asymptotically $l_0^* \to l_{0\,\mathrm{min}}$ and simultaneously $\bar{l}_0 \to l_0^*$, for $R \to \infty$. One may not perform the expansion of $\frac{\partial H(l_0,R)}{\partial l_0}$ around the value of l_0 which corresponds to $\alpha = \pi$, as this value is smaller than l_0^* for finite R (see figure 4).

Instead, one expands $\frac{\partial H(l_0,R)}{\partial l_0}$ around $l_0^{(0)} = l_0^*$, which fulfils

$$\tau_1 + (\tau_1 + 2b\mathrm{e}^{-l_0^{(0)}/\xi_\mathrm{B}}) \cos[\alpha(l_0^{(0)}, R)] = 0. \tag{3.1}$$

The solution of equation (3.1) takes—for $\frac{\sigma\xi_\mathrm{B}}{\tau_1 R} \ll 1$—the following form:

$$\mathrm{e}^{-l_0^{(0)}/\xi_\mathrm{B}} = \frac{\sigma\pi^2\xi_\mathrm{B}^2}{2\tau_1 R^2}\left(1 - 2\frac{\sqrt{2\sigma b}}{\tau_1}\frac{\xi_\mathrm{B}}{R} + \frac{1}{2}(6 - \pi^2/2)\frac{2\sigma b}{\tau_1^2}\frac{\xi_\mathrm{B}^2}{R^2} + \mathcal{O}\left(\frac{\sigma\xi_\mathrm{B}}{\tau_1 R}\right)^3\right). \tag{3.2}$$

Similarly, by expanding $\frac{\partial H(l_0,R)}{\partial l_0}$ around the above value $l_0^{(0)}$, we solve the equation $\frac{\partial H(l_0,R)}{\partial l_0} = 0$ up to terms of the order $(\frac{\xi_\mathrm{B}\sigma}{\tau_1 R})^4$. In this way one obtains the equilibrium droplet height

$$\mathrm{e}^{-\bar{l}_0/\xi_\mathrm{B}} = \frac{\sigma\pi^2\xi_\mathrm{B}^2}{2\tau_1 R^2}\left(1 + \frac{\kappa_1}{R} + \frac{\kappa_2}{R^2} + \mathcal{O}\left(\left(\frac{\sigma\xi_\mathrm{B}}{\tau_1 R}\right)^3\right)\right), \tag{3.3}$$

where

$$\kappa_1 = \xi_B\sqrt{8\sigma b}\frac{2\tau_1-\tau_2}{\tau_1\tau_2},$$
$$\kappa_2 = 8\sigma b\xi_B^2\left[\frac{6-\frac{\pi^2}{2}}{8\tau_1^2}+\frac{2}{\tau_2^2}-\frac{2}{\tau_1\tau_2}-\frac{-2\tau_1^3+5\tau_1^2\tau_2-2\tau_1\tau_2^2+\tau_2^3}{\tau_1\tau_2^2(2\tau_1^2-3\tau_1\tau_2+\tau_2^2)}\right].$$

If in equation (3.3) one neglects the correction terms of the order $\sim\left(\frac{\sigma\xi_B}{\tau_1 R}\right)^3$ and $\sim\left(\frac{\sigma\xi_B}{\tau_1 R}\right)^4$, then one recovers the result obtained by Parry *et al* via conformal transformation [31].

The droplet height

$$\bar{l_0} = \xi_B\left[\log\left(\frac{2\tau_1 R^2}{\pi^2\sigma\xi_B^2}\right)-\frac{\kappa_1}{R}-\frac{\kappa_2-\frac{1}{2}\kappa_1^2}{R^2}+\cdots\right]$$

exhibits logarithmic divergence for $R\to\infty$. The first correction ($\sim 1/R$) is positive. Both κ_1 and κ_2 depend on b and thus cannot be obtained within the conformal scheme [31]. Note that the asymptotic expansion was performed while keeping τ_i ($i=1,2$) constant. Taking the limits $\xi_B/R\to 0$ and $\tau_i/\sigma\to 0$ are non-commutative operations and—consequently—the above expansion (3.3) is valid only provided $\frac{\xi_B\sigma}{R\tau_1}\ll 1$. This remark also remains relevant for the cases $\tau_1=0$ and $\tau_1<0$ discussed below.

3.2. The $\tau_1 = 0$ regime

The plot of the function $H(l_0, R)$ for $\tau_1=0$ case is qualitatively similar to the $\tau_1>0$ case; see figure 4. However, in the present case the quantity $\bar{l}_0$ corresponds to $\alpha(\bar{l}_0(R))\to\frac{\pi}{2}^-$ for $R\to\infty$. Hence, we may expand $H(l_0, R)$ around $l_0^{(0)}$, which fulfils the condition $\alpha(l_0^{(0)}, R)=\pi/2$. After solving the equation $\frac{\partial H(l_0,R)}{\partial l_0}=0$ we obtain

$$\mathrm{e}^{-\bar{l}_0/\xi_B} = \sqrt{\frac{\sigma}{2b}}\frac{\pi}{2}\frac{\xi_B}{R}\left(1+\frac{\gamma_1}{R}+\frac{\gamma_2}{R^2}+\mathcal{O}\left(\left(\frac{\xi_{\|2}}{R}\right)^3\right)\right), \tag{3.4}$$

where $\gamma_1=-2\xi_{\|2}$, $\gamma_2=4\xi_{\|2}^2$. The explicit expression for $\bar{l}_0$ has the form

$$\bar{l}_0 = \xi_B\left[\log\sqrt{\frac{2b}{\sigma}}\frac{2}{\pi}\frac{R}{\xi_B}+\frac{2\xi_{\|2}}{R}-\frac{2\xi_{\|2}^2}{R^2}+\cdots\right].$$

The leading correction term, as for the case $\tau_1>0$, is positive.

3.3. The $\tau_1 < 0$ regime

Our first observation concerning the case $\tau_1<0$ is that, in the limit $R\to\infty$, the equilibrium droplet height $\bar{l}_0(R)$ converges to a finite value $l_{\pi 1}$ corresponding to the minimum of the potential $V_1(l)$. Indeed, as the inhomogeneity size becomes infinite, the height of the drop at its centre is fully determined by the properties of substrate type 1. The quantity $l_0^{(0)}=l_{\pi 1}$ is therefore a natural choice of the value around which $\frac{\partial H(l_0,R)}{\partial l_0}$ can be expanded for large R. Note that unlike the former cases $\tau_1\geqslant 0$, the effective potential $V_1(l_0)$ becomes negative close to $l_0=\bar{l}_0(R)\simeq l_{\pi 1}$ and so the formula in equation (2.10) should be used instead of (2.11). Solving $\frac{\partial H(l_0,R)}{\partial l_0}=0$ up to the relevant order leads to

$$\bar{l}_0 = l_{\pi 1}+\delta_1\mathrm{e}^{-R/\xi_{\|1}}+\delta_2\mathrm{e}^{-2R/\xi_{\|1}}+\mathcal{O}(\mathrm{e}^{-3R/\xi_{\|1}}), \tag{3.5}$$

where $\delta_1=2\xi_B\frac{\tau_1-\tau_2}{\tau_1+\tau_2}$, and $\delta_2=\frac{1}{2}\delta_1^2/\xi_B$. The leading correction is negative and equal to 0 for the special case $\tau_1=\tau_2$, as is expected on physical grounds.

To sum up the results obtained for the morphology of the liquid drop we note that the form of the $\bar{l}_0$ expansion for large R depends crucially on the value of the reduced temperature τ_1. For $\tau_1 \geqslant 0$, which corresponds to complete wetting of type 1 substrate, one has corrections proportional to powers of $1/R$, while for $\tau_1 < 0$ we obtain corrections proportional to powers of $\mathrm{e}^{-R/\xi_{\parallel 1}}$.

4. The line tension

The expressions for the line tension $\eta(R) = H(\bar{l}_0, R)$ are obtained by substituting the formulae for $\bar{l}_0$ into equations (2.10) and (2.11). The calculations are rather cumbersome and we refrain from quoting the expressions for η in terms of the parameters of the expansion of $\bar{l}_0(R)$ around $R = \infty$. We only note that the leading R-independent term in η may be expressed in terms of the parameters κ_1, γ_1 or δ_1 for all cases $\tau_1 > 0$, $\tau_1 = 0$, $\tau_1 < 0$, respectively. The next-to-leading corrections in $\bar{l}_0$ modify η at the level of leading R-dependent terms.

We obtain the following expressions:

$$\eta_{>}(R, \tau_1, \tau_2) = \xi_{\mathrm{B}}\sqrt{\frac{\sigma}{2b}}\left[\tau_1 \log\left(\frac{\tau_1 - \tau_2}{\tau_1}\right) - \tau_2 \log\left(\frac{2(\tau_2 - \tau_1)}{\tau_2}\right)\right] - \sigma\xi_{\mathrm{B}}\left[\frac{\pi^2}{2}\frac{\xi_{\mathrm{B}}}{R} + \mathcal{O}\left(\left(\frac{\xi_{\mathrm{B}}}{R}\right)^2\right)\right], \tag{4.1}$$

for $\tau_1 > 0$,

$$\eta_0(R, \tau_1, \tau_2) = -\xi_{\mathrm{B}}\tau_2\sqrt{\frac{\sigma}{2b}}\log(2) - \sigma\xi_{\mathrm{B}}\left[\frac{\pi^2}{8}\frac{\xi_{\mathrm{B}}}{R} + \mathcal{O}\left(\left(\frac{\xi_{\mathrm{B}}}{R}\right)^2\right)\right], \tag{4.2}$$

for $\tau_1 = 0$, and finally

$$\eta_{<}(R, \tau_1, \tau_2) = \xi_{\mathrm{B}}\sqrt{\frac{\sigma}{2b}}\left[\tau_1 \log\left(\frac{\tau_1 + \tau_2}{2\tau_1}\right) + \tau_2 \log\left(\frac{\tau_1 + \tau_2}{2\tau_2}\right)\right] + \xi_{\mathrm{B}}\tau_1\sqrt{\frac{\sigma}{2b}}\left[-2\frac{\tau_1}{\tau_1 + \tau_2}\mathrm{e}^{-R/\xi_{\parallel 1}} + \mathcal{O}\left(\frac{R}{\xi_{\mathrm{B}}}\mathrm{e}^{-2R/\xi_{\parallel 1}}\right)\right], \tag{4.3}$$

for $\tau_1 < 0$.

The dominant, R-independent terms in the above formulae may be obtained independently by considering an inhomogeneous substrate consisting of two homogeneous half-planes characterized by τ_1, τ_2, meeting at $x = 0$. After calculating the corresponding excess linear free energy one obtains the dominant, R-independent term. It is a non-negative function of τ_1 and τ_2, which vanishes for $\tau_1 = \tau_2$; see figure 5.

The central observation concerning the above formulae is the change in the character of the corrections to the 'free' line tension $\eta^{(0)}$ as the temperature $T_{\mathrm{W}1}$ is crossed. The interfacial correlation length $\xi_{\parallel 1} = \xi_{\mathrm{B}}\frac{\sqrt{2\sigma b}}{|\tau_1|}$ sets the length scale controlling the next-to-leading terms in $\eta_{<}$, i.e., for $\tau_1 < 0$. Its divergence at $\tau_1 = 0$ is accompanied by the appearance of the algebraic terms in the expansion of η about $1/R = 0$ for $\tau_1 \geqslant 0$. The finite R corrections for $\tau_1 > 0$ are universal (at least up to $\sim 1/R$ order) in the sense that they do not depend on the substrates' characteristics and are fully determined by σ. Thus the divergence of $\xi_{\parallel 1}$ at $\tau_1 = 0$ is accompanied by the change of the expansion parameter of η from $\mathrm{e}^{-R/\xi_{\parallel 1}}$ to ξ_{B}/R.

The corrections are positive for $\tau_1 < 0$ and negative for $\tau_1 \geqslant 0$. They may be interpreted as the asymptotic term of an effective interaction potential between two regions of inhomogeneity of $\bar{l}(x)$, corresponding to $x \sim R$ and $x \sim -R$.

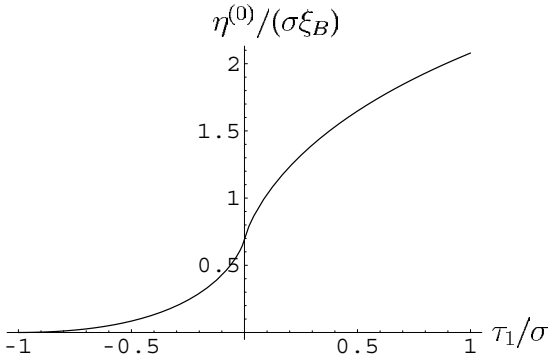

Figure 5. Plot of the leading R-independent contribution to the line tension denoted by $\eta^{(0)}$ as function of τ_1 at fixed τ_2. The plot parameters were chosen as follows: $\sigma/2b = -\tau_2/2b = 1$. Note that for $\tau_1 = \tau_2$ one has $\eta^{(0)} = 0$ as expected on physical grounds. The range of τ_1 is restricted to $\tau_1 > \tau_2$ in accordance with the analysis in the text.

It is worth noting that the leading R-dependent contribution to the line tension was studied numerically for $\tau_1 < 0$ in the case of long-range intermolecular forces in [8]. This quantity was shown to be positive (as in our case) and to decay as R^{-2} in the limit $R \to \infty$.

5. Remarks on the contact angles

At the macroscopic level the contact angle of a liquid drop placed on a planar solid surface is related to the interfacial tensions between the relevant phases. Accordingly, it can be evaluated from Young's equation [18]. Within the mesoscopic description the three-phase contact line is not defined unambiguously, and consequently the geometric construction of the contact angle is not unique. Moreover, generalizations of Young's equation to the case of chemically inhomogeneous substrates assume implicitly that the typical size of boundary regions between homogeneous domains is much larger than the bulk correlation length ξ_{B} (see [7] for detailed discussion), which is opposite to the case considered in this paper.

There are at least two approaches towards the geometric definition of the contact angle for the system considered in this paper. The first definition exploits the interfacial profile's characteristics in the region of an inhomogeneity (i.e., for $|x| \approx R$) while the second probes the profile's features at the centre of the droplet (i.e. for $x \approx 0$), and corresponds to a phenomenological construction of the contact angle commonly applied in different contexts (see e.g. [28, 30, 34]).

Within the first approach the equilibrium contact angle is defined via the profile's slope at the three-phase contact line situated at a chosen position x_k. A natural—though not unique—choice for the considered system is $x_k = R$. Hence, the contact angle θ is obtained from

$$\tan\theta = -\left.\frac{\mathrm{d}\bar{l}(x)}{\mathrm{d}x}\right|_{x=R}. \tag{5.1}$$

In the second approach one fits the circle $y(x) = \sqrt{\mathcal{R}^2 - x^2} + y_0$, tangent to $\bar{l}(x)$ at $x = 0$, and of the same curvature at $x = 0$ as that of $\bar{l}(x)$: $\frac{\mathrm{d}^2 y(x)}{\mathrm{d}x^2}|_{x=0} = -\frac{1}{\mathcal{R}} = \frac{\mathrm{d}^2\bar{l}(x)}{\mathrm{d}x^2}|_{x=0}$. The position of the contact line is then defined as the line of intersection of $y(x)$ with the profile's asymptote at $l_{\pi 2}$; see figure 6.

Within the present analytical approach the above two constructions can be achieved only in the case of large inhomogeneity width $R/\xi_{\parallel 1} \gg 1$. For the first choice

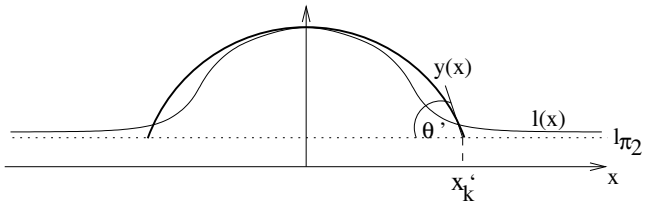

Figure 6. Phenomenological construction of the contact line and the contact angle. A circle $y(x)$ fitted to the equilibrium droplet profile at $x = 0$ intersects the asymptote $l_{\pi 2}$ at x_k' defining the three-phase contact line position. The contact angle θ' is defined as the corresponding angle of intersection.

one obtains

$$\theta \simeq \begin{cases} \dfrac{1}{2}(\theta_2 - \theta_1) & \text{for } \tau_1 \leqslant 0 \\ \dfrac{1}{2}\dfrac{\theta_2^2}{\frac{\tau_1}{\sqrt{2\sigma b}} + \theta_2} & \text{for } \tau_1 > 0, \end{cases} \tag{5.2}$$

where θ_1 and θ_2 are the contact angles for homogeneous substrates of type 1 and 2, respectively, and for small, negative τ_i one has $\theta_i \simeq |\tau_i|/\sqrt{2\sigma b}$, $i = 1, 2$.

It is obvious on physical grounds that the second construction leads for $R/\xi_{\parallel 1} \gg 1$ to a vanishing contact angle. This is confirmed by the analytical expressions

$$\theta' \simeq \begin{cases} 2|\tau_1|\sqrt{(l_{\pi 1} - l_{\pi 2})\dfrac{\tau_2 - \tau_1}{\tau_1 + \tau_2}\dfrac{1}{2\sigma b}}\,\mathrm{e}^{-\frac{1}{2}R/\xi_{\parallel 1}} & \text{for } \tau_1 < 0 \\ \dfrac{\pi}{\sqrt{2}}\dfrac{\sqrt{\log[-(2/(\sigma b))^{1/2}\tau_2 R/\pi]}}{R} & \text{for } \tau_1 = 0 \\ \pi\dfrac{\sqrt{\log\left[\frac{\tau_1\tau_2 R^2}{-\pi^2\sigma b}\right]}}{R} & \text{for } \tau_1 > 0, \end{cases} \tag{5.3}$$

which display a change of the convergence type to the value $\theta'(R = \infty) = 0$ from exponential for $\tau_1 < 0$ to $\frac{\sqrt{\log(R)}}{R}$ for $\tau_1 \geqslant 0$. In other words, the discrepancy between our predictions for θ and θ' may be attributed to the different behaviour of the corresponding positions x_k and x_k' of the contact line for $R \to \infty$. In particular, the difference $x_k - x_k'$ is of the order $\mathrm{e}^{R/(2\xi_{\parallel 1})}$ for $\tau_1 < 0$ and $\sqrt{\log R}$ for $\tau_1 \geqslant 0$.

Let us also note that the concept of contact angle is useful in the limit of macroscopic droplet size only. Consequently, the above constructions of the quantities θ and θ' are valid for $R \to \infty$ in the case $\tau_1 \geqslant 0$, while within the temperature range $\tau_1 < 0$ the additional assumption $-\tau_1/b \ll 1$ (corresponding to $l_{\pi 1} \approx \bar{l_0} \to \infty$) must be made. To reach the macroscopic droplet regime in the case $\tau_1 < 0$ consistently with the procedure of obtaining the droplet height $\bar{l_0}$ (see section 3) the limits $\tau_1 \to 0^-$, $R \to \infty$ must be performed, bearing in mind the condition $\frac{R}{\xi_{1\parallel}} = -\frac{R\tau_1}{\xi_B\sqrt{2\sigma b}} \gg 1$.

We sum up with the statement that the superficially appealing semicircle construction, successfully applied in different contexts (see [28, 30, 34]) in the present case of volatile liquid droplet stabilized by a chemical substrate heterogeneity, leads to a rather meaningless notion of the contact angle.

6. Summary

This article is concerned with the morphology and line tension of equilibrium droplets placed on a planar substrate with a chemical, stripe-shaped inhomogeneity.

Applying the effective Hamiltonian approach, we first constructed a set of constrained equilibrium states parameterized by the droplet height. The global minimum was then extracted from this set using a perturbative expansion valid in the limit of large droplet radii. The line tension expressions were evaluated and the character of the size-dependent correction shown to exhibit crossover from exponential to algebraic decay for increasing inhomogeneity's width, occurring at the stripe's wetting temperature. This corresponds to divergence of the interfacial correlation length characterizing the wetted part of the surface, which acts as the length scale controlling the line tension for low temperatures.

In addition, on the basis of the obtained equilibrium liquid–vapour profiles $\bar{l}(x)$ we calculated the droplet contact angle on the heterogeneous substrate defined via tangents of $\bar{l}(x)$ evaluated at $x = R$.

The main conclusions are restricted to the case of short-ranged forces and refer to the asymptotic regime $R/\xi_{\parallel 1} \to \infty$, and the thermodynamic state close to the fluid two-phase coexistence ($\mu = \mu_{\mathrm{sat}}^{-}$). Our predictions are as follows.

- The line tension η related to the substrate's inhomogeneity is a function of the stripe's width R. For large R the character of the leading R-dependent term depends on the temperature. At low temperatures, i.e., for $T < T_{\mathrm{W}1}$, the interfacial correlation length $\xi_{\parallel 1}$ represents the characteristic length scale controlling the R-dependent contributions to line tension, which are of the type $\mathrm{e}^{-R/\xi_{\parallel 1}}$. For $T \geqslant T_{\mathrm{W}1}$ the correlation length $\xi_{\parallel 1}$ is infinite, and the R-dependent contributions to η become algebraic and universal, i.e. independent of the substrates' properties, and fully determined by the liquid–vapour interfacial tension σ.
- The R-dependent contributions to η may be interpreted as the effective interaction potential between the interfacial profile inhomogeneity regions corresponding to droplet boundaries at $x \approx R$ and $x \approx -R$. At $T = T_{\mathrm{W}1}$ the leading R-dependent correction to η changes sign from positive in the low temperature regime $T < T_{\mathrm{W}1}$ to negative for $T \geqslant T_{\mathrm{W}1}$. This means that the interaction represented by these terms is repulsive as long as T does not exceed $T_{\mathrm{W}1}$ and attractive for $T > T_{\mathrm{W}1}$. The interaction magnitude is governed by the inverse of the correlation length $1/\xi_{\parallel 1} = |\tau_1|/\sqrt{2\sigma b}$ for $T < T_{\mathrm{W}1}$ and by the interfacial tension σ in the case of $T \geqslant T_{\mathrm{W}1}$.
- In order to characterize the interfacial morphology in terms of the contact angle we analysed two definitions of the contact angle. They turn out to be highly sensitive to the choice of the three-phase contact line. A particular choice of this line positioned at the domain boundary leads to a contact angle expressible in terms of contact angles on homogeneous substrates. Another choice, inspired by experimental procedures and based on droplets' properties at their centres, leads—in the present context—to contact angles asymptotically (for $R \to \infty$) equal to 0 for all temperatures.

Acknowledgment

The support by the Committee for Scientific Research grant KBN 2P03B 008 23 is gratefully acknowledged.

References

[1] Hauge E 1992 *Phys. Rev.* A **46** 4994
[2] Rejmer K, Dietrich S and Napiórkowski M 1999 *Phys. Rev.* E **60** 4027
[3] Parry A, Rascón C and Wood A 1999 *Phys. Rev. Lett.* **83** 5535
[4] Parry A, Rascón C and Wood A 2000 *Phys. Rev. Lett.* **85** 345
[5] Drelich J, Wilbur J, Miller J and Whitesides G 1996 *Langmuir* **12** 1913
[6] Urban D, Topolski K and De Coninck J 1996 *Phys. Rev. Lett.* **76** 4388
[7] Swain P and Lipowsky R 1998 *Langmuir* **14** 6772
[8] Bauer C and Dietrich S 1999 *Phys. Rev.* E **60** 6919
[9] Dietrich S and Bauer C 2000 *Phys. Rev.* E **62** 2428
[10] Lenz P, Bechinger C, Schafle C, Leiderer P and Lipowsky R 2001 *Langmuir* **17** 7814
[11] Lenz P and Lipowsky R 1998 *Phys. Rev. Lett.* **80** 1920
[12] Swain P and Lipowsky R 2000 *Europhys. Lett.* **80** 203
[13] Hołyst R and Poniewierski A 1987 *Phys. Rev.* B **36** 5628
[14] Indekeu J, Upton P and Yeomans J 1988 *Phys. Rev. Lett.* **61** 2221
[15] Netz R and Andelman D 1997 *Phys. Rev.* E **55** 687
[16] Rejmer K and Napiórkowski M 1997 *Z. Phys.* B **102** 101
Rejmer K and Napiórkowski M 1997 *Phys. Rev.* E **62** 588
[17] Rascón C and Parry A 2000 *J. Phys.: Condens. Matter* **12** A369
[18] Rowlinson R and Widom B 1982 *Molecular Theory of Capillarity* (New York: Oxford University Press)
[19] Widom B and Clarke A 1990 *Physica* A **168** 149
[20] Indekeu J 1992 *Physica* A **183** 439
[21] Varea C and Robledo A 1992 *Phys. Rev.* A **45** 2645
[22] Abraham D, Latrémoliére F and Upton P 1993 *Phys. Rev. Lett.* **71** 404
[23] Indekeu J and Robledo A 1993 *Phys. Rev.* E **47** 4607
[24] Indekeu J 1994 *Int. J. Mod. Phys.* B **8** 309
[25] Koch W, Dietrich S and Napiórkowski M 1995 *Phys. Rev.* E **51** 3300
[26] Getta T and Dietrich S 1998 *Phys. Rev.* E **57** 655
[27] Pompe T and Herminghaus S 1999 *Phys. Rev.* E **83** 3677
[28] Wang J, Betelu S and Law B 2001 *Phys. Rev.* E **63** 031601
[29] Pompe T 2002 *Phys. Rev. Lett.* **89** 076102
[30] Checco A, Guenoun P and Dailland J 2003 *Phys. Rev. Lett.* **91** 186101
[31] Parry A, Macdonald E and Rascón C 2001 *J. Phys.: Condens. Matter* **13** 383
[32] Bauer C, Dietrich S and Parry A 1999 *Europhys. Lett.* **47** 474
[33] Bauer C and Dietrich S 1999 *Eur. Phys. J.* B **10** 767
[34] Dobbs H 1999 *Int. J. Mod. Phys.* B **13** 3255